Large Amplitude Motions in 2,3-Dimethylfluorobenzene: Steric Effects Failing to Interpret Hindered Methyl Torsion

Safa Khemissi, Arnau Pérez Salvador, Ha Vinh Lam Nguyen

Large Amplitude Motions in 2,3-Dimethylfluorobenzene: Steric Effects Failing to Interpret Hindered Methyl Torsion

Safa Khemissi,[a] *Arnau Pérez-Salvador,*[a] *and Ha Vinh Lam Nguyen*[a,b]*

[a] Univ Paris Est Creteil and Université de Paris, CNRS, LISA, F-94010 Créteil, France

[b] Institut Universitaire de France (IUF), F-75231 Paris, France

* Corresponding author. Email: lam.nguyen@lisa.ipsl.fr

GRAPHICAL ABSTRACT

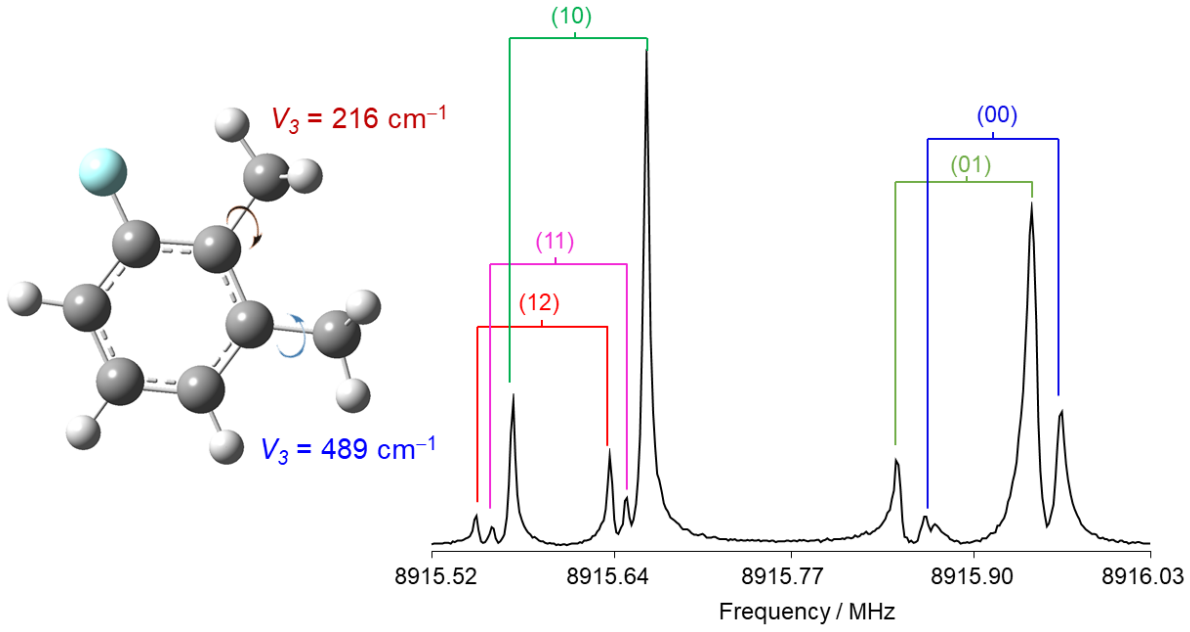

ABSTRACT

The microwave spectrum of 2,3-dimethylfluorobezene, one of the six isomers of dimethylfluorobenzene, was recorded using a pulsed molecular jet Fourier transform microwave spectrometer operating in the frequency range from 2 to 26.5 GHz. The internal rotations of two inequivalent methyl groups, causing splittings of up to several hundred MHz of all rotational energy levels into quintets, were analyzed and modeled. The torsional barriers of the methyl groups at the *ortho* and the *meta* positions were determined to be 215.5740(56) cm^{-1} and 488.53(11) cm^{-1}. A comparison with the barrier heights observed for the two isomers 2,6-dimethylfluorobenzene and 3,4-dimethylfluorobenzene has shown that the methyl group at the *meta* position seems to be invisible to its neighboring *ortho*-methyl group, while the *meta*-methyl group clearly senses the *ortho* one. Steric effects are not able to explain this observation, and electrostatic effects are most probably the reason. Highly accurate molecular parameters determined experimentally were compared with those obtained from quantum chemical calculations at different levels of theory.

INTRODUCTION

Large Amplitude Motion (LAM), featuring several types such as ring puckering,[1] inversion tunneling,[2] and internal rotation,[3] has been a classic topic in microwave spectroscopy along its whole history for over a century. The spectrum of a LAM containing molecule includes additional splittings, and is much more complicated than in the case of a rigid-rotor molecule. Among all types of LAM, methyl internal rotation is probably the most intensively studied.[3] In the rotational spectrum, each rotational line splits into an A and an E species for a one-top case. This so-called A-E splitting depends on a characteristic parameter, the barrier to internal rotation. Generally, the higher the torsional barrier, the smaller the A-E splitting and vice versa.

In a molecule featuring two methyl rotors, all rotational lines split into quintets in the case of two inequivalent methyl groups, or quartets for two equivalent ones.[3]

LAM containing molecules with conjugated π-double bonds are of special interest as electronic effects can be transferred across a longer range, often enabling interactions between two internal rotors. The reason for the value of a methyl torsional barrier is often answered by steric effects. In molecules where obviously no steric hindrance can occur, for example when a methyl group is separated to the frame by a C≡C-bond, almost free internal rotation with a very low torsional barrier of less than 10 cm^{-1} was observed, as in the case of, i.e., 4-hexyn-3-ol,[4] 3-pentyn-1-ol,[5] 1-chloro-2-butyne,[6] 2-butynoic acid,[7] and tetrolyl fluoride.[8] When a methyl group is located next to a group or an atom, steric hindrance occurs and the methyl torsional barrier increases to an intermediate value between about 400 – 600 cm^{-1}, as observed in 3,4-dimethylbenzaldehyde,[9] 1,2-dimethylnapthalene,[10] 3,4-dimethylfluorobenzene,[11] 2-chloro-4-fluorotoluene,[12] 2-halogenotoluene,[13] or *o*-methylanisole .[14] While it is evident to expect whether steric effects may occur, electrostatic effects sometimes cause unexpected values for the methyl torsional barriers. The barrier height of 26.9 cm^{-1} found for the *o*-methyl group in 2,3-dimethylanisole,[15] or that of 126.5 cm^{-1} for the 4-methyl group and of 61.7 cm^{-1} for the 5-methyl group of 4,5-dimethylthiazole[16] are surprisingly low. Those methyl groups are sterically hindered, so that a barrier of lower than 100 cm^{-1} cannot be explained by steric effects. Electrostatic effects come into question, but there are not enough data points to support any assumption.

The closely related structure between 2,3-dimethylanisole (molecule (**1**) in Figure 1) and 2,3-dimethylfluorobenzene (**2**, 23DMFB) induced us to study the title compound where the *o*-methyl group is also sterically hindered by a methyl group on one side and a fluorine atom on the other side. In the dimethylfluorobenzene family, the microwave spectra of the 2,6-[17] and 3,4-isomers[11] have been reported and serve as good reference points for the present study on

23DMFB. In 3,4-dimethylfluorobenzene (**4**, 34DMFB), steric hindrance between the two neighboring methyl groups is clearly responsible for intermediate torsional barriers of both methyl tops. In the case of the 2,6-isomer (**3**, 26DMFB), steric effects can also explain the barrier height of 237 cm^{-1} of the two equivalent methyl rotors. Because a methyl group is bulkier than a fluorine atom, steric hindrance for the *o*-methyl group in 26DMFB (**3**) is lower than that for the two methyl groups in 34DMFB (**4**), causing consequently a lower torsional barrier in 26DMFB (**3**). With this knowledge, one tends to assume on the one hand that the *meta*-methyl group in 23DMFB (**2**) would experience the same steric hindrance as that of the two methyl groups in 34DMFB (**4**) and thus would possess the same torsional barrier. This is finally a correct assumption. On the other hand, the *o*-methyl group of 23DMFB (**2**) is sterically hindered by a methyl group on one side and by a fluorine atom on the other side. Therefore, it should overcome a barrier height of even larger than that of the *meta*-methyl group. The present experimental work, supported by quantum chemical calculations, eventually proves this assumption to be wrong and shows that steric effects fail completely to explain the torsional barrier of the *o*-methyl group in 23DMFB (**2**).

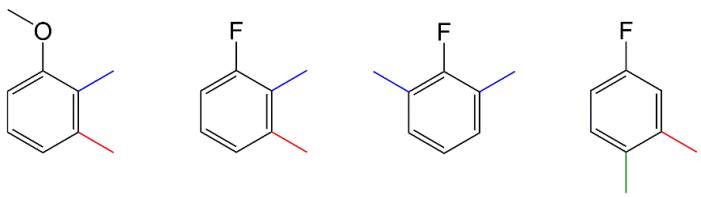

Figure 1. Comparison of the torsional barriers of the *o*- and *m*-methyl groups in 23DMFB with those of 2,3-dimethylanisole and two other isomers in the dimethylfluorobenzene family: (**1**) 2,3-dimethylanisole,[15] (**2**) 2,3-dimethylfluorobenzene (this work), (**3**) 2,6-dimethylfluorobenzene,[17] (**4**) 3,4-dimethylfluorobenzene.[11] The torsional barriers are given in cm^{-1} and are color-coded.

THEORETICAL METHODS

The rotational constants were predicted by geometry optimizations at three levels of theory using the program *Gaussian 16*.[18] Three levels of theory, B3LYP-D3BJ/6-311++G(d,p), MP2/6-311++G(d,p), and MP2/6-31G(d,p), which have been benchmarked for the 2,6- and 3,4-isomers,[11,17] are also applied to study 23DMFB. The equilibrium rotational constants A_e, B_e, C_e and dipole moment components are summarized in Table 1. Ground state rotational constants A_0, B_0, C_0 and centrifugal distortion constants are calculated by anharmonic frequency calculations at the B3LYP-D3BJ/6-311++G(d,p) and MP2/6-311++G(d,p) levels. The geometry of 23DMFB optimized at the B3LYP-D3BJ/6-311++G(d,p) level is shown in Figure 2. The atomic Cartesian coordinates are given in Table S1; important bond lengths and angles in Table S2 of the Supporting Information.

In our previous studies on 26DMFB and 34DMFB,[11,17] benchmark calculations using a vast number of method-basis set combinations recommend B3LYP-D3BJ/6-311++G(d,p) as a suitable level whose error compensations accidentally yield good agreement between the calculated equilibrium rotational constants and the experimental ground state constants. As we shall see in the results and discussion section, calculations at the three levels of theory mentioned above provide quite satisfactory results. As an effort to continue our benchmarks, we repeat the geometry optimizations of 23DMFB at different levels of theory as those used for 26DMFB and 34DMFB, employing several Pople[19] and Dunning[20] basis sets in combination with the MP2[21] and CCSD[22] *ab initio* methods, as well as some density functional theory (DFT) methods. They are the above mentioned B3LYP[23,24] including Grimme's dispersion corrections (D3)[25] with or without Becke-Johnson damping (BJ),[26] Truhlar's M06-2X,[27] and Head-Gordon's ωB97X-D functionals.[28] The B3LYP functional was also combined with the Coulomb-attenuating method (CAM).[29] For the ωB97X-D functional, a combination with the

6-31G(d) basis set was applied in addition, as recommended by a recent benchmark work by Lee and McCarthy.[30] The obtained results are listed in Table S3 of the Supporting Information.

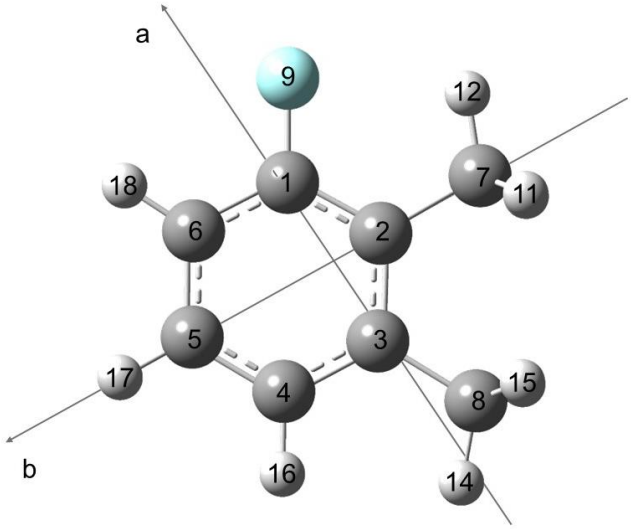

Figure 2. Molecular structure of 23DMFB as optimized at B3LYP-D3BJ/6-311++G(d,p) level of theory.

Table 1. Equilibrium rotational constants A_e, B_e, C_e (in MHz) and dipole moment components (in D) of 23DMFB.

	B3LYP-D3BJ/ 6-311++G(d,p)	MP2/ 6-311++G(d,p)	MP2/ 6-31G(d,p)
A_e	2243.3	2230.6	2240.6
B_e	1737.2	1731.4	1734.7
C_e	991.0	986.8	989.6
A_0	2228.4	2212.9	
B_0	1724.1	1717.1	
C_0	984.0	978.5	
μ_a	1.81	1.92	−1.72
μ_b	0.14	0.58	0.64
μ_c	0.00	0.01	0.00

Due to internal rotation of two inequivalent methyl groups, splittings into quintets are expected for all rotational transitions. According to the notation given in Ref. [31] based on the semi-direct product $(C_3^I \otimes C_3^I) \leftthreetimes C_s$, the torsional species will be labeled as ($\sigma_1\sigma_2$) = (00), (01), (10), (11), and (12) with σ_1 and σ_2 referring to the *ortho* and the *meta* methyl group, respectively.

The barriers heights of the two inequivalent methyl rotors at the *ortho* and *meta* positions were calculated at the three levels of theory aforementioned by varying the dihedral angles α_1 = ∠(C_1,C_2,C_7,H_{12}) and α_2 = ∠(C_4,C_3,C_8,H_{14}), respectively, (for atom numbering, see Figure 2) in a grid of 10° for 12 steps to obtain a rotation of 120° respecting the threefold symmetry of the methyl groups. All other geometry parameters were optimized. The potential energy curves for both methyl groups are shown in Figure 3. The torsional barriers predicted at the B3LYP-D3BJ/6-311++G(d,p), MP2/6-311++G(d,p), and MP2/6-31G(d,p) levels of theory are 196.4 cm^{-1}, 140.8 cm^{-1}, and 167.1 cm^{-1}, respectively, for the methyl group at the *ortho* position, and 444.9 cm^{-1}, 453.3 cm^{-1}, and 423.9 cm^{-1} for that in the *meta* position.

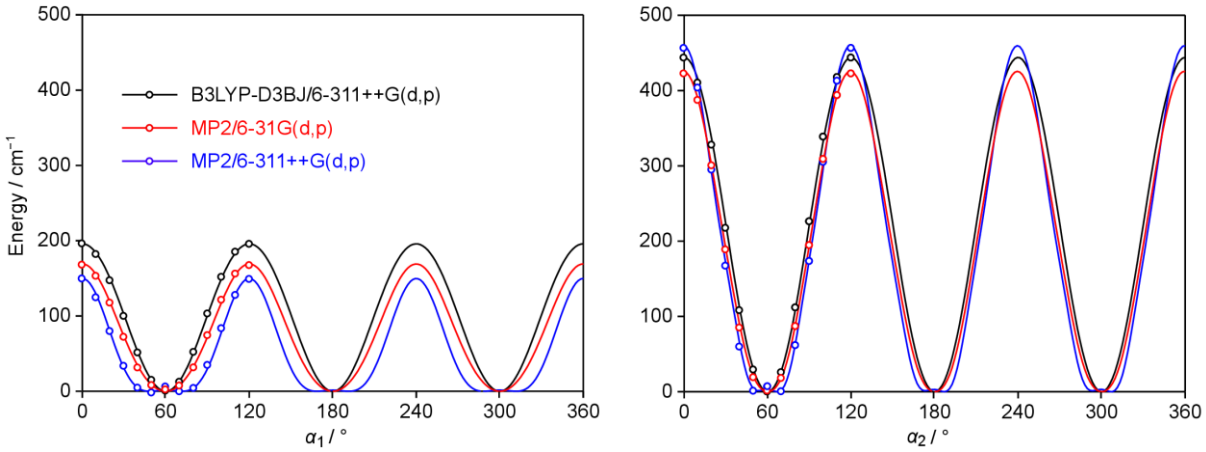

Figure 3. Three-fold potential energy curves calculated by varying the dihedral angles α_1 = ∠(C_1,C_2,C_7,H_{12}) and α_2 = ∠(C_4,C_3,C_8,H_{14}), corresponding to the internal rotation of the *o*- and *m*-methyl groups, respectively. For each methyl group, calculations were performed at the B3LYP-D3BJ/6-

311++G(d,p) (black curve), MP2/6-311++G(d,p) (blue curve), and MP2/6-31G(d,p) (red curve) levels of theory.

We also calculated the two-dimensional (2D) potential energy surface (PES) depending on the dihedral angles α_1 and α_2 to study the coupling of the *o*- and *m*-methyl tops. The two dihedral angles were varied in grid of 10°, and all other geometry parameters were optimized at the B3LYP-D3BJ/6-311++G(d,p) level of theory. The PES was parameterized with a 2D-Fourier expansion as follow:

$$V(\alpha) = -410.26428\, Hartree + \frac{229.2\ cm^{-1}}{2} cos(3\alpha_1) - \frac{474.2\ cm^{-1}}{2} cos(3\alpha_2) - 14.7\ cm^{-1} \cdot cos(3\alpha_1)cos(3\alpha_2) + 38.8\ cm^{-1} \cdot sin(3\alpha_1)sin(3\alpha_2). \quad (1)$$

If only the Fourier V_3 terms cos(3α_1) and cos(3α_2) are fitted together with a constant term, we obtain a maximal deviation of 7.4% of all data points within the dynamic range, which slightly decreases to 6.1% if the two V_6 terms are included. Fitting in addition the cos(α_1)·cos(α_2) term was sufficient in the cases of 26DMFB and 34DMFB, but in 23DMFB, no change in the deviation was observed. Instead, the sin(α_1)·sin(α_2) term seems to influence much more the data set. Fitting this term together with the V_3 terms decreases the deviation to 4.0%. Including the cos(α_1)·cos(α_2) term in addition, as given in Eq. (1), yields an acceptable maximal deviation of 1.9%. From the PES, we determined a V_3 term of 229.2 cm^{-1} for the *o*-methyl and 474.2 cm^{-1} for the *m*-methyl group. The values of the Fourier terms cos(α_1)·cos(α_2) and sin(α_1)·sin(α_2) indicate that there is significant coupling between the *o*- and *m*-methyl groups. Similar results were obtained with calculations at the MP2/6-311++G(d,p) and MP2/6-31G(d,p) levels, as shown in Figure S1 of the Supporting Information.

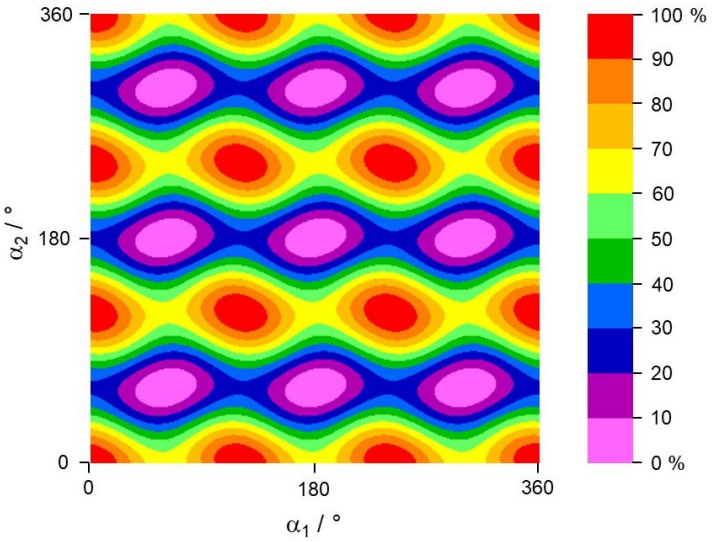

Figure 4. The 2D-PES of 23DMFB depending on the dihedral angles α_1 and α_2 calculated at the B3LYP-D3BJ/6-311++G(d,p) level of theory. The numbers in the color code indicate the energy in percent relative to the energetic minimum E_{min} = −410.2658322 Hartree (0%) and the energetic maximum E_{max} = −410.2626474 Hartree (100%).

EXPERIMENTAL SECTION

Measurements. A sample of 23DMFB was purchased from TCI Europe, Zwijndrecht, Belgium, indicating a purity of 98 %, and used without further purification. A few drops of 23DMFB were put on a piece of a pipe cleaner placed in front of the nozzle. Under helium stream at a backing pressure of 2 bar, the 23DMFB-helium mixture was expanded into the vacuum chamber.

The microwave spectrum was recorded using a pulsed jet Fourier transform spectrometer operating in the frequency range from 2 to 26.5 GHz.[32] First, a broadband scan was recorded from 10.7 to 12.9 GHz. Subsequently, all observed lines were remeasured at a higher resolution with an example given in Figure 5. Due to the Doppler effect, the lines appear as doublets because of the co-axial arrangement between the molecular beam and the

resonators. After the spectrum had been assigned, new lines outside of the scan could be measured from 2.7 GHz to 22.8 GHz directly in the high resolution mode. Line broadening was observed in the high-resolution spectra of 23DMFB, probably due to unresolved spin-spin or spin-rotation splittings. The measurement accuracy is estimated to be about 4 kHz, whereas the experimental accuracy achievable in the high-resolution mode of the spectrometer is about 2 kHz.[33]

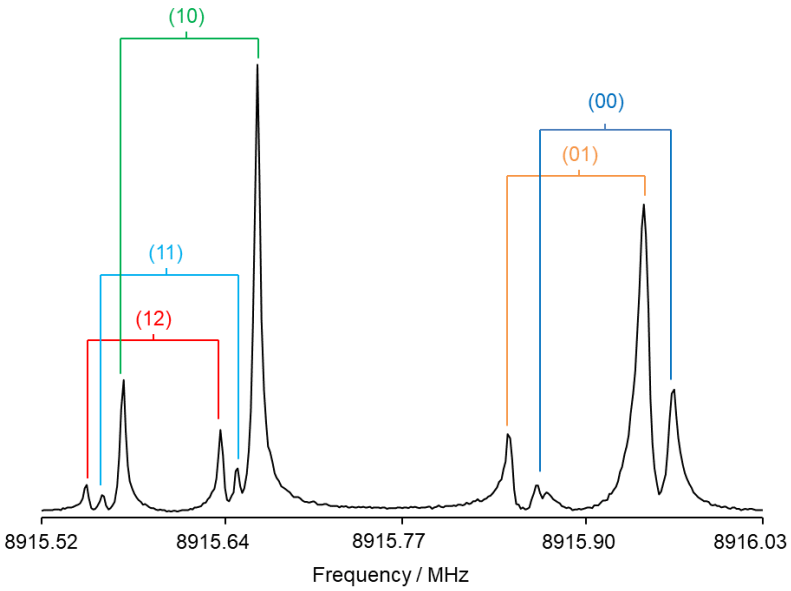

Figure 5. A typical spectrum of the *a*-type transition $4_{04} \leftarrow 3_{03}$ of 23DMFB recorded at high resolution which splits into five torsional components (00), (01), (10), (11), and (12). The Doppler doublets are marked by brackets.

Spectrum assignments and fits. At the beginning, the internal rotations of the *o*- and *m*-methyl groups were neglected, and we considered 23DMFB as an effective rigid rotor. According to the calculated dipole moment components given in Table 1, *b*-type transitions should be much less intense than *a*-type ones. The rigid rotor spectrum was predicted with the program *XIAM*[34] using rotational constants calculated at the B3LYP-D3BJ/6-311++G(d,p) level. The intense *a*-type *R*-branch $5_{05} \leftarrow 4_{05}$, $5_{14} \leftarrow 4_{13}$, $6_{06} \leftarrow 5_{05}$, and $6_{16} \leftarrow 5_{15}$ transitions were first assigned and

fitted, yielding accurate values for the *B* and *C* rotational constants. Further *a*-type lines could be measured straightforwardly. We then searched for *b*-type transitions and found a small number of them, which enabled accurate determination of the *A* rotational constant.

The high resolution spectra revealed clumps of transitions arising from the internal rotations of the two inequivalent methyl groups. In a second step, a prediction was carried out considering these large amplitude motions. From the predicted splittings, the (01), (10), (11), and (12) torsional species could be easily assigned. In total, 391 torsional species lines were identified and included in a global *XIAM* fit. The rotational constant F_0 of the two methyl groups was constrained to 158.0 GHz. The angles $\angle(i_1,a)$ and $\angle(i_2,a)$ between the *a*-axis and the rotation axes of the two tops as well as the two barrier heights $V_{3,1}$ and $V_{3,2}$ were fitted together with the three rotational constants, three quartic centrifugal distortion constants D_J, d_1, d_2, and three higher order parameters $D_{p_i^2 J}$, $D_{p_i^2 K}$, $D_{p_i^2 -}$ for the *o*-methyl rotor, giving a standard deviation of 3.6 kHz. To check the correctness of the assigned frequencies, each torsional species was fitted separately with the program *SFLAMS* (Separately Fitting of Large Amplitude Motion Species)[35] using the odd power parameters *q* and *r* required for the (01), (10), (11), and (12) species. They multiply the angular momentum components $\mathbf{P_a}$ and $\mathbf{P_b}$, respectively, which change sign under the time-reversal operation, making the Hamiltonian effective. On the other hand, they contain numerical expectation values of the torsional angular momentum operators $\mathbf{p_\alpha}$ of the methyl groups, being also of odd order. If included in the Hamiltonian explicitly under time reversal, $\mathbf{p_\alpha}$ would also change sign as $\mathbf{P_a}$ and $\mathbf{P_b}$. The sign changes cancel out, and the odd power terms become invariant as they should be.[36] These terms are not necessary to fit separately the (00) species, which follows a semi-rigid rotor Hamiltonian model. The standard deviations obtained for the (00), (01), (01), (11), and (12) species are close to 4 kHz, confirming that all frequencies are correctly assigned and the measurement accuracy is about 4 kHz. The results of the five separate fits are summarized in Table 2; those of the *XIAM* global fit in Table

3. A list of all fitted frequencies along with their residuals obtained with the program *XIAM* is given in Table S4 of the Supporting Information, available also as an ASCII text file. Interestingly, in the separate fits of the (10), (11), and (12) species, associating with the lower barrier *o*-methyl rotor (215.6 cm^{-1}, see Table 3), the *r* parameter, multiplying $\mathbf{P_b}$, dominates the *q* parameter, multiplying $\mathbf{P_a}$, i.e., *r* is much larger than *q*. In the (11) fit, *q* was not necessary to achieve a satisfactory fit. We also note that *r* increases by almost 30 times from fit (01) to the other fits, since (01) refers to the higher barrier *m*-methyl rotor (488.5 cm^{-1}). Therefore, the (01) line frequencies require smaller correction to be fitted separately than the (10), (11), and (12) species do. For example, a very large *r* value of 1.2 GHz was determined for the E species of 3-pentyn-1-ol because of the very low barrier of 10 cm^{-1} of the propynyl methyl group.[3,5]

Table 2. Molecular parameters obtained by fitting separately the (00), (01), (10), (11), and (12) torsional species with the *SFLAMS* program.

Par.[a]	**Unit**	**Fit (00)**	**Fit (01)**	**Fit (10)**	**Fit (11)**	**Fit (12)**
A	MHz	2240.32576(34)	2240.28837(35)	2240.32572(56)	2240.28907(63)	2240.28997(73)
B	MHz	1739.49778(23)	1739.49307(25)	1738.47812(29)	1738.47270(32)	1738.47260(44)
C	MHz	991.089073(87)	991.089013(89)	991.090413(85)	991.090548(97)	991.09025(10)
D_J	kHz	0.0684(18)	0.0705(19)	0.01140(55)	0.01169(63)	0.01046(62)
D_{JK}	kHz			0.185(12)	0.161(14)	0.375(42)
D_K	kHz			0.116(29)	0.174(32)	−0.309(93)
d_1	kHz	0.02839(87)	0.02973(92)			
d_2	kHz	0.0720(47)	0.0773(50)	0.0463(64)	0.0343(71)	0.129(21)
q	MHz		1.6353(10)	1.62409(98)		3.387(21)
r	MHz		1.78(23)	52.224(11)	52.833(12)	51.602(17)
N[b]		80	80	79	79	73
σ[c]	kHz	3.7	3.8	3.6	4.1	3.9

[a] All parameters refer to the principal axis system. Watson's S reduction in the I^r representation was used. Standard errors in parentheses are in the unit of the least significant digits. [b] Number of lines. [c] Standard deviation of the fit.

Table 3. Molecular parameters of 23DMFB obtained in a global fit with the *XIAM* program.

Par.[a]	Unit	Fit *XIAM*	Calc.[b]
A	MHz	2240.30023(19)	2243.322
B	MHz	1738.81664(13)	1737.173
C	MHz	991.078651(43)	991.004
D_J	kHz	0.05900(73)	0.11387
d_1	kHz	–0.02872(51)	–0.00734
d_2	kHz	–0.00493(18)	–0.00009
$V_{3,1}$	cm^{-1}	215.5740(56)	196.4
$V_{3,2}$	cm^{-1}	488.53(11)	444.9
$D_{p_i^2 J,1}$	MHz	0.03663(38)	
$D_{p_i^2 K,1}$	MHz	–0.0519(13)	
$D_{p_i^2 -,1}$	MHz	0.03229(37)	
$\angle(i_1,a)$[c]	°	88.6190(10)	90.28
$\angle(i_1,b)$	°	178.6190(10)	179.72
$\angle(i_2,a)$	°	154.53(14)	151.86
$\angle(i_2,b)$	°	115.47(14)	118.14
N[d]		391	
σ[e]	kHz	3.6	

[a] All parameters refer to the principal axis system. Watson's S reduction in I^r representation was used. Standard errors in parentheses are in the unit of the least significant digits. Rotors 1 and 2 refer to the *o*- and *m*-methyl groups, respectively. [b] Values of the equilibrium structure calculated at the B3LYP-D3BJ/6-311++G(d,p) level of theory. Centrifugal distortion constants obtained by anharmonic frequency calculations, D_{JK} = –0.17197 kHz, D_K = 0.06935 kHz. [c] $\angle(i,c)$ is fixed to 90° due to symmetry. [d] Number of lines. [e] Standard deviation of the fit.

After assigning the spectrum of 23DMFB, we did not find any unassigned lines in the survey spectrum that could be of ^{13}C isotopologue origin. From our experiences in other molecules of the dimethylfluorobenzene family,[11,17] the isotopologue lines are too weak to be observed with the scan mode of the spectrometer in use, partly due to splittings arising from the internal rotations of two methyl groups which decrease the line intensity. Since the present study does not focus on structure determination, we did not intensively search for the isotopologues of 23DMFB.

RESULTS AND DISCUSSION

The program *XIAM* was used to fit 391 torsional transitions in the microwave spectrum of 23DMFB to a standard deviation of 3.6 kHz which is the estimated measurement accuracy. The rotational constants calculated at the B3LYP-D3BJ/6-311++G(d,p) level of theory are in very good agreement with the experimental values (see Table 3). Rotational constants calculated at all other levels of theory given in Table S3 also agree well in general. We found excellent match for the *A* rotational constant in calculations at the at MP2/6-31G(d,p) level of theory, for the *B* and *C* rotational constants with B3LYP-D3BJ in combination with two basis sets 6-311++G(d,p) and 6-311+G(d,p). The ωB97X-D functional in combination with Dunning's cc-pVDZ basis set and Pople's 6-31G(d) basis set recommended in Ref. [30] also provides very satisfactory results. Overall, regarding also the results for the two isomers 26DMFB[17] and 34DMFB,[11] the B3LYP-D3BJ/6-311++G(d,p) level of theory yields values of equilibrium rotational constants B_e which are in almost exact agreement with the experimental B_0 values. It is obvious that from theoretical perspective, the B_e constants should not be compared with the B_0 constants. But benefiting from error compensations which accidentally work well for a certain class of molecules to access good starting values of the rotational constants to guide the assignment has become a common way in the practice. The potential barriers of the *o*- and *m*-methyl groups calculated at the B3LYP-D3BJ/6-311++G(d,p) level are in good agreement with the experimental values (see Table 3).

The barrier height of 488.53(11) cm^{-1} observed for the *m*-methyl group in 23DMFB is extremely close to the value of 490 cm^{-1} found for the *p*-methyl group in 34DMFB and also close to the slightly lower value of 456 cm^{-1} of the *m*-methyl group of 34DMFB.[11] This can be explained by steric effects as the steric surrounding of the *m*-methyl group in 23DMFB and the *p*-methyl group in 34DMFB is only a methyl group. On the other hand, the torsional barrier of 216 cm^{-1} of the *o*-methyl group of 23DMFB remains almost the same as (or more precisely,

even lower than) that in 2-fluorotoluene,[13] 26DMFB[17] (237 cm^{-1} in both molecules), or 2-fluoro-4-chlorotoluene (230 cm^{-1})[37] where only a fluorine atom is located next to the methyl group. The methyl group at the *m*-position seems to be "invisible" for the *o*-methyl group, but results from the 2D-PES calculations suggest a strong coupling between them. This can only be explained by electrostatic interaction. Assuming that a methyl group and a fluorine atom are similar, then the *o*-methyl group would experience a six-fold potential arising from a C_{2v} frame symmetry and the C_{3v} symmetry of the methyl group. Then, only a small V_6 term would exist. But certainly, a methyl group and a fluorine atom are by far not similar. Therefore, a V_3 potential is dominant, however, the torsional barrier is still affected. The same observation was found for the *o*-methyl group in 2,3-dimethylanisole with an even lower torsional barrier of only 27 cm^{-1},[15] almost by an order of magnitude lower than for the *o*-methyl group of 23DMFB. Probably, the electronic surrounding of the O-CH_3 group of 2,3-dimethylanisole is more similar to that of a methyl group than that of a fluorine atom. Currently, we do not have a conclusive proof for this statement, except the observation that if a methyl group is squashed between two groups/atoms, there is a high possibility to discover unexpectedly low torsional barriers for which steric effects fail to explain. Examples known for instance are 23DMFB (this work, the methyl group between a fluorine atom and a methyl group), 2,3-dimethylanisole (27 cm^{-1}, the methyl group between a methoxy group and a methyl group), [15] 4,5-dimethylthiazole (127 cm^{-1} and 62 cm^{-1}, the methyl groups between a methyl group and a sulfur or a nitrogen atom, respectively),[16] and 2-methylthiazole (35 cm^{-1}, the methyl group between a sulfur and a nitrogen atom).[38] Further similar systems are aimed in the future to yield valuable inputs to understand the origin of this interesting effect.

CONCLUSION

The microwave spectrum of 23DMFB measured under molecular jet conditions was successfully assigned. The internal rotations of the two inequivalent methyl groups in the *ortho* and *para* positions cause splittings of each rotational transition into five torsional species which were observed and fitted using the program *XIAM* to a standard deviation close to the measurement accuracy. Separately fitting of each torsional species was performed to check the assignment. The rotational constants calculated at different levels of theory are in good agreement with the experimental values, and the B3LYP-D3BJ/6-311++G(d,p) level remains the recommended one for the dimethylfluorobenzene family. By comparing the barrier heights of the methyl torsions to those observed for the two isomers 26DMFB and 34DMFB as well as other molecules, we found that steric effects fail to explain the much lower value found for the *o*-methyl group, and electrostatic effects are suggested to be the reason.

ASSOCIATED CONTENT

Supporting Information. Potential energy surfaces depending on the dihedral angles α_1 and α_2 calculated at MP2/6-311++G(d,p) and MP2/6-31G(d,p) levels of theory, nuclear coordinates, bond lengths, and bond angles of the optimized structure, basis set variation, and frequency lists. Tables of the basis set variations and frequency lists also available as ASCII text files.

AUTHOR INFORMATION

Corresponding Author

*Ha Vinh Lam Nguyen, lam.nguyen@lisa.ipsl.fr

Author Contributions

The manuscript was written through contributions of all authors. All authors have given approval to the final version of the manuscript.

ACKNOWLEDGEMENTS

We thank Prof. Dr. Marie-Claire Gazeau for her support in the Erasmus bachelor thesis of A.P.-S. at LISA. This work was supported by the Agence Nationale de la Recherche ANR (project ID ANR-18-CE29-0011).

REFERENCES

(1) Legon, A. C. Equilibrium Conformations of Four- and Five-Membered Cyclic Molecules in the Gas Phase: Determination and Classification. *Chem. Rev. 1980*, **80**, 231–262.

(2) Nguyen, H. V. L.; Gulaczyk, I.; Kręglewski, M.; Kleiner, I. Large Amplitude Inversion Tunneling Motion in Ammonia, Methylamine, Hydrazine, and Secondary Amines: From Structure Determination to Coordination Chemistry. *Coord. Chem. Rev.* **2021**, *436*, 213797.

(3) Nguyen, H. V. L.; Kleiner, I. Understanding (Coupled) Large Amplitude Motions: The Interplay of Microwave Spectroscopy, Spectral Modeling, and Quantum chemistry. *Phys. Sci. Rev.* [Online] 2021, *6*. DOI: 10.1515/psr-2020-0037

(4) Eibl, K.; Stahl, W.; Kleiner, I.; Nguyen, H. V. L. Conformational Effect on the Almost Free Internal Rotation of 4-Hexyn-3-ol Studied by Microwave Spectroscopy and Quantum Chemistry. *J. Chem. Phys.* **2018**, *149*, 144306.

(5) Eibl, K.; Kannengießer, R.; Stahl, W.; Nguyen, H. V. L.; Kleiner, I. Low Barrier Methyl Rotation in 3-Pentyn-1-ol as Observed by Microwave Spectroscopy. *Mol. Phys.* **2016**, *114*, 3483–3489.

(6) Stolwijk, V. M.; van Eijck. B. P. Microwave Spectrum and Barrier to Internal Rotation of 1-Chloro-2-butyne. *J. Mol. Spectrosc.* **1987**, *124*, 92–98.

(7) Ilyushin, V.; Rizzato, R.; Evangelisti, L.; Feng, G.; Maris, A.; Melandri, S.; Caminati, W. Almost Free Methyl Top Internal Rotation: Rotational Spectrum of 2-Butynoic Acid. *J. Mol. Spectrosc.* **2011**, *267*, 186–190.

(8) Hensel, K. D.; Gerry, M. C. L. Microwave Spectrum of Tetrolyl Fluoride. *J. Chem. Soc., Faraday Trans.* **1994**, *90*, 3023–3027.

(9) Tudorie, M.; Kleiner, I.; Jahn, M.; Grabow, J.-U.; Goubet, M.; Pirali, O. Coupled Large Amplitude Motions: A Case Study of the Dimethylbenzaldehyde Isomers. *J. Phys. Chem. A.* **2013**, *117*, 13636–13647.

(10) Schnitzler, E. G.; Zenchyzen, B. L. M.; Jäger, W. High-Resolution Fourier-Transform Microwave Spectroscopy of Methyl- and Dimethylnapthalenes. *Astrophys. J.* **2015**, *805*, 141.

(11) Mélan, J.; Khemissi, S.; Nguyen, H. V. L. Steric Effects on Two Inequivalent Methyl Internal Rotations of 3,4-Dimethylfluorobenzene. *Spectro. Chem. Acta A.* **2021**, *253*, 119564.

(12) Nair, K. P. R.; Herbers, S.; Bailey, W. C.; Obenchain, D. A.; Lesarri, A.; Grabow, J.-U.; Nguyen, H. V. L. Internal Rotation and Chlorine Nuclear Quadrupole Coupling in 2-Chloro-4-fluorotoluene Explored by Microwave Spectroscopy and Quantum Chemistry. *Spectrochim. Acta A.* **2020**, *247*, 119120.

(13) Herbers, S.; Buschmann, P.; Wang, J.; Lengsfeld, K. G.; Nair, K. P. R.; Grabow, J.-U. Reactivity and Rotational Spectra: The Old Concept of Substitution Effects. *Phys. Chem. Chem. Phys.* **2020**, *22*, 11490−11497.

(14) Ferres, L.; Mouhib, H.; Stahl, W.; Nguyen, H. V. L. Methyl Internal Rotation in the Microwave Spectrum of *o*-Methyl Anisole. *ChemPhysChem*. **2017**, *18*, 1855−1859.

(15) Ferres, L.; Truong, K.-N.; Stahl, W.; Nguyen, H. V. L. Interplay Between Microwave Spectroscopy and X-ray Diffraction: The Molecular Structure and Large Amplitude Motions of 2,3-Dimethylanisole. *ChemPhysChem*. **2018**, *19*, 1781−1788.

(16) Van, V.; Nguyen, T.; Stahl, W.; Nguyen, H. V. L.; Kleiner, I. Coupled Large Amplitude Motions: The Effects of Two Methyl Internal Rotations and ^{14}N Quadrupole Coupling in 4,5-Dimethylthiazole Investigated by Microwave Spectroscopy. *J. Mol. Struct.* **2020**, *1207*, 127787.

(17) Khemissi, S.; Nguyen, H. V. L. Two Equivalent Internal Rotations in the Microwave Spectrum of 2,6-Dimethylfluorobenzene. *ChemPhysChem*. **2020**, *21*, 1682−1687.

(18) Frisch, M. J.; Trucks, G. W.; Schlegel, H. B.; Scuseria, G. E.; Robb, M. A.; Cheeseman, J. R.; Scalmani, G.; Barone, V.; Petersson, G. A.; Nakatsuji, H., et al. *Gaussian 16*, Revision B.01; Gaussian, Inc., Wallingford CT, 2016.

(19) Frisch, M. J.; Pople, J. A.; Binkley, J. S. Self-Consistent Molecular Orbital Methods 25. Supplementary Functions for Gaussian Basis Sets. *J. Chem. Phys.* **1984**, *80*, 3265−3269.

(20) Dunning Jr., T. H. Gaussian Basis Sets for Use in Correlated Molecular Calculations. I. The Atoms Boron Through Neon and Hydrogen *J. Chem. Phys.* **1989**, *90*, 1007−1023.

(21) Møller, C.; Plesset, M. S. Note on an Approximation Treatment for Many-Electron Systems. *Phys. Rev.* **1934**, *46*, 618−622.

(22) Bartlett, R. J.; Musial, M. Coupled-Cluster Theory in Quantum Chemistry. *Rev. Mod. Phys.* 2007, 79, 291–352.

(23) Becke, A. D. Density-Functional Thermochemistry. III. The Role of Exact Exchange. *J. Chem. Phys.* **1993**, *98*, 5648−5652.

(24) Lee, C. T.; Yang, W. T.; Paar, R. G. Development of the Colle-Salvetti Correlation-Energy Formula into a Functional of the Electron Density. *Phys. Rev. B* **1988**, *37*, 785−789.

(25) Grimme, S.; Antony, J.; Ehrlich, S.; Krieg, H. A Consistent and Accurate ab initio Parametrization of Density Functional Dispersion Correction (DFT-D) for the 94 Elements H-Pu. *J. Chem. Phys.* **2010**, *132*, 154104.

(26) Grimme, S.; Ehrlich, S.; Goerigk, L. Effect of the Damping Function in Dispersion Corrected Density Functional Theory. *J. Comput. Chem.* **2011**, *32*, 1456−1465.

(27) Zhao, Y.; Truhlar, D. G. The M06 Suite of Density Functionals for Main Group Thermochemistry, Thermochemical Kinetics, Noncovalent Interactions, Excited States, and Transition Elements: Two New Functionals and Systematic Testing of Four M06-Class Functionals and 12 Other Functionals. *Theor. Chem. Acc.* **2008**, *120*, 215−241.

(28) Chai, J.-D.; Head-Gordon, M. Long-Range Corrected Hybrid Density Functionals with Damped Atom-Atom Dispersion Corrections. *Phys. Chem. Chem. Phys.* **2008**, *10*, 6615−6620.

(29) Yanai, T., Tew, D. P., Handy, N. C. A New Hybrid Exchange–Correlation Functional Using the Coulomb-Attenuating Method (CAM-B3LYP). *Chem. Phys. Lett.* **2004**, *393*, 51−57.

(30) Lee, K. L. K; McCarthy, M. Bayesian Analysis of Theoretical Rotational Constants from Low-Cost Electronic Structure Methods. J. Phys. Chem. A 2020, 124, 898-910.

(31) Ferres, L.; Cheung, J.; Stahl, W.; Nguyen, H. V. L. Conformational Effect on the Large Amplitude Motions of 3,4-Dimethylanisole Explored by Microwave Spectroscopy. *J. Phys. Chem. A.* **2019**, *123*, 3497−3503.

(32) Grabow, J.-U.; Stahl W.; Dreizler, H. A Multioctave Coaxially Oriented Beam-Resonator Arrangement Fourier Transform Microwave Spectrometer. *Rev. Sci. Instrum*. **1996**, *67*, 4072−4084.

(33) Grabow, J.-U.; Stahl, W. A Pulsed Molecular Beam Microwave Fourier Transform Spectrometer with Parallel Molecular Beam and Resonator Axes. *Z. Naturforsch*. **1990**, *45a*, 1043−1044.

(34) Hartwig, H.; Dreizler, H. The Microwave Spectrum of *Trans*-2,3-Dimethyloxirane in Torsional Excited States. *Z. Naturforsch*. **1996**, *51a*, 923−932.

(35) Herbers, S.; Fritz, S. M.; Mishra, P.; Nguyen, H. V. L.; Zwier, T. S. Local and Global Approaches to Treat the Torsional Barriers of 4-Methylacetophenone Using Microwave Spectroscopy. *J. Chem. Phys.* **2020**, *152*, 074301.

(36) Ohashi, N.; Hougen, J. T.; Suenram, R.; Lovas, F.; Kawashima, Y.; Fujitake, M.; Pyka, J. Analysis and Fit of the Fourier-Transform Microwave Spectrum of the Two-Top Molecule *N*-Methylacetamide. *J. Mol. Spectrosc.* **2004**, *227*, 28–42.

(37) Nair, K. P. R.; Herbers, S.; Grabow, J.-U.; Nguyen, H. V. L. Neighborhood Matters: Steric Effects on Methyl Internal Rotation and Chlorine Nuclear Quadrupole Coupling in 2-Fluoro-4-chlorotoluene. *J. Mol. Struct.* **2021**, *1246*, 131096.

(38) Nguyen, T.; Van, V.; Gutlé, C.; Stahl, W.; Schwell, M.; Kleiner, I.; Nguyen, H. V. L. The Microwave Spectrum of 2-Methylthiazole: ^{14}N Nuclear Quadrupole Coupling and Methyl Internal Rotation. *J. Chem. Phys.* **2020**, *152*, 134306.